Environmental Science & Technology

pubs.acs.org/est

Article

Effects of Metal Ions on Aqueous-Phase Decomposition of α-Hydroxyalkyl-Hydroperoxides Derived from Terpene Alcohols

Mingxi Hu, Kenichi Tonokura, Yu Morino, Kei Sato, and Shinichi Enami*

Cite This: *Environ. Sci. Technol.* 2021, 55, 12893−12901

Read Online

ACCESS | Metrics & More | Article Recommendations | Supporting Information

ABSTRACT: We report the results of a mass spectrometric study of the effects of atmospherically relevant metal ions on the decomposition of α-hydroxyalkyl-hydroperoxides (α-HHs) derived from ozonolysis of α-terpineol in aqueous solutions. By direct mass spectrometric detection of chloride adducts of α-HHs, we assessed the temporal profiles of α-HHs and other products in the presence of metal ions. In addition, reactions between α-HHs and $FeCl_2$ in the presence of excess DMSO showed that the amount of hydroxyl radicals formed in a mixture of α-terpineol, O_3, and $FeCl_2$ was 5.7 ± 0.8% of the amount formed in a mixture of H_2O_2 and $FeCl_2$. The first-order rate constants for the decay of α-HHs produced by ozonolysis of α-terpineol in the presence of 5 mM acetate buffer at a pH of 5.1 ± 0.1 were determined to be (4.5 ± 0.1) × 10^{-4} s^{-1} (no metal ions), (4.7 ± 0.2) × 10^{-4} s^{-1} (with 0.05 mM Fe^{2+}), (4.7 ± 0.1) × 10^{-4} s^{-1} (with 0.05 mM Zn^{2+}), and (4.8 ± 0.2) × 10^{-4} s^{-1} (with 0.05 mM Cu^{2+}). We propose that in acidic aqueous media, the reaction of α-HHs with Fe^{2+} is outcompeted by H^+-catalyzed decomposition of α-HHs, which produces the corresponding aldehydes and H_2O_2, which can in turn react with Fe^{2+} to form hydroxyl radicals.

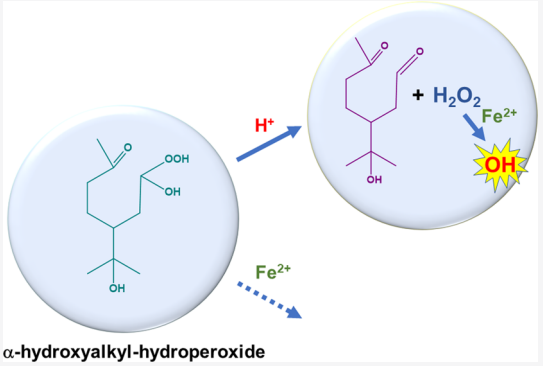

α-hydroxyalkyl-hydroperoxide

KEYWORDS: *peroxides, Fenton reaction, Fenton-like reactions, reactive oxygen species, OH radical, Criegee intermediates*

1. INTRODUCTION

Atmospheric oxidation of volatile organic compounds by both hydroxyl (OH) radicals and ozone produces organic hydroperoxides (ROOHs), which are taken up into atmospheric condensed phases such as aqueous aerosols, secondary organic aerosols (SOAs), and cloud/fog droplets.[1] Because ROOHs are highly reactive, they are expected to contribute to changes in the oxidative and toxicological potentials of atmospheric particulate matter. Atmospheric model simulations have predicted that ROOHs account for up to 60% of global SOAs.[2] In addition, ROOHs play critical roles in environmental, advanced oxidation, and biological processes.[3]

Among the most important ROOHs in the atmosphere are α-hydroxyalkyl-hydroperoxides (α-HHs), which have a −OOH group and a −OH group attached to the same carbon atom. α-HHs are major products of the ozonolysis of volatile organic compounds in the presence of water vapor. In particular, α-HHs are generated by reactions between $(H_2O)_{n\geq 1}$ and diradical/zwitterion carbonyl oxides (Criegee intermediates, CIs) formed by ozonolysis of alkenes. Although the atmospheric fate of CIs strongly depends on their chemical structure,[4−6] the overwhelming abundance of water vapor in the atmosphere favors their reaction with $(H_2O)_{n\geq 1}$. For example, at relative humidity (RH) = 50% (i.e., $[H_2O]$ = 3.8 × 10^{17} molecule cm^{-3} and $[(H_2O)_2]$ = 3.0 × 10^{14} molecule cm^{-3}), $(H_2O)_2$ could convert CH_2O_2 (the smallest CI) into hydroxymethyl hydroperoxide (the smallest α-HH) within 0.5 ms.[4] Moreover, multiphase ozonolysis of alkenes in the presence of water also produces α-HHs as major products.[7−9] Because of the hydrophilicity and large Henry's law constants of α-HHs (e.g., the constant for hydroxymethyl-hydroperoxide is 5.0 × 10^5 M atm^{-1} at 295 K),[10] these compounds are expected to reside mostly in condensed phases such as fog/cloud droplets, aqueous aerosols, and SOAs in the atmosphere. Recent studies revealed that liquid-phase α-HHs decompose to the corresponding aldehydes and H_2O_2 at a rate that depends sensitively on the water content, pH, and temperature of the reaction solution.[1] In particular, pH (a measure of $[H^+]$) strongly determines the lifetimes of α-HHs derived from α-terpineol (α-Tp) and terpinen-4-ol in aqueous phases. We found that not only these α-HHs but also α-alkoxyalkyl hydroperoxides possessing a −OOH group and a −OR' group generated from the reaction of α-Tp CIs with C_1−C_3 alcohols decompose via an H^+-catalyzed mechanism in aqueous phases.[11] It is important to note that atmospheric condensed

Received: July 12, 2021
Published: September 16, 2021

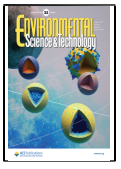

phases are acidic by nature,[12] and H^+-catalyzed reactions can therefore be expected to play essential roles in the fate of terpene-derived α-HHs and α-alkoxyalkyl hydroperoxides.[1]

Whether the reactions of α-HHs with coreactants can compete with H^+-catalyzed reactions has not been explored. Metal ions such as Fe^{2+}, Zn^{2+}, Cu^{2+}, and Fe^{3+} are ubiquitous in atmospheric condensed phases; and Fe^{2+} and Fe^{3+}, which are water-soluble, are known to play central roles in many atmospheric, environmental, and biological processes.[13] Typical concentrations of Fe^{2+} in cloud and rain water are reported to be ~0.05 μM (marine), 0.5 μM (remote), and 5 μM (urban).[14] A model simulation study predicted that the $[Fe^{2+}]/[Fe^{3+}]$ ratio in cloud droplets differs between day and night because solar photolysis of Fe^{3+} complexes converts Fe^{3+} into Fe^{2+}.[14] Zn^{2+} influences the hygroscopicity of aerosol particles by forming complexes with oxalate,[15] and Cu^{2+} plays key roles in the HO_x chemistry in cloud/fog droplets.[14,16] The typical concentrations of ROOHs in cloud droplets and rain water are ~3.9 μM (marine), 20 μM (remote), and 0.5 μM (urban).[17] Thus, α-HHs are expected to coexist with metal ions in atmospheric aqueous phases at similar concentrations (i.e., ≤20 μM).

A previous experimental study indicated that methyl hydroperoxide (CH_3OOH) and ethyl hydroperoxide (C_2H_5OOH) in the presence of Fe^{2+} in water at pH 2 decompose to produce the corresponding alkoxy (RO) radicals rather than OH radicals.[17] The rate constants for reactions of these hydroperoxides with Fe^{2+} at 279 K and pH 2 were 16 ± 5 and 24 ± 9 M^{-1} s^{-1}, respectively. These values are comparable with the value for the reaction of H_2O_2 with Fe^{2+} (the Fenton reaction). In addition to a direct reaction between ROOHs and metal ions, various metal-catalyzed reactions have also been reported.[18]

Herein, we report the first mass spectrometric investigation of the effects of atmospherically relevant metal ions on the decomposition of α-HHs derived from terpene alcohols in water. We compared the yields of OH radicals from mixtures of α-HHs and Fe^{2+} and mixtures of H_2O_2 and Fe^{2+}. In addition, we used two different pH buffers to determine the rate constants for α-HH decay in the absence and presence of Fe^{2+}, Zn^{2+}, Cu^{2+}, and Fe^{3+}. We found that H^+-catalyzed decomposition of α-HHs was much faster than a direct reaction of α-HHs with metal ions or metal-catalyzed decomposition of α-HHs. We suggest that the pH of the reaction medium, rather than the presence of these metal ions, determines the fate of α-HHs derived from α-Tp and terpinen-4-ol and probably other terpenes as well.

2. MATERIALS AND METHODS

The experimental setup and procedure used in this study were essentially the same as those reported previously.[19−21] α-Tp or terpinen-4-ol (2 mM) and NaCl (0.4 mM) were dissolved in 10 mL of Milli-Q water in a 25 mL glass vial (Figure S1). These terpene alcohols were chosen because of their high water solubilities (~15 mM; for comparison, the solubility of α-pinene is 0.018 mM) and because they are oxygenated volatile organic compounds detected in the atmosphere and in indoor environments.[22] Separately, aqueous O_3 solutions were prepared by sparging water (10 mL) in a 25 mL vial for 20 s with O_3(g) generated by means of a commercial ozonizer (KSQ-050, Kotohira, Japan) fed with ultrahigh-purity O_2(g) (>99.999%). The initial O_3 concentration in the solutions, $[O_3(aq)]_0$, was 0.06 ± 0.01 mM, as determined with a UV−vis spectrometer (Agilent 8453) using the reported O_3 molar extinction coefficient at 258 nm (ε_{258nm} = 3840 M^{-1} cm^{-1} in water[23]).

Ozonolysis reactions were initiated by mixing the solution of α-Tp and NaCl and the O_3 solution (10 mL each) in a 25 mL glass vial (Figure S1). Then, an $FeCl_2$ solution (50 μL) was added using a micropipette, and the reaction mixture was stirred. For pH-controlled experiments, either an acetate buffer (pH 5.1) or a phosphate buffer (pH 7.6) was added to the reaction mixtures. The pH values of the reaction mixtures were measured with a calibrated pH meter (LAQUA F-74, Horiba) during the measurement. The $[\alpha\text{-Tp}]_0/[O_3(aq)]_0$ ratio was maintained at ~17 to avoid unwanted secondary reactions; under these conditions, O_3 was consumed exclusively by α-Tp ($[\alpha\text{-Tp}]_0$ = 1 mM, k = 9.9 × 10^6 M^{-1} s^{-1}) within a lifetime ($\tau_{1/e}$) of ~0.1 ms.[22] Note that [α-HH] was always less than $[O_3]_0$ (= 0.06 mM) and was close to ambient [ROOH] values (0.5−20 μM) in atmospheric aqueous phases.[17]

Next, a glass syringe (5 mL, covered with an aluminum foil to avoid photodegradation) and a syringe pump (Pump 11 Elite, Harvard Apparatus) were used to immediately inject the reaction mixture (100 μL min^{-1}) into an electrospray mass spectrometer (Agilent 6130 quadrupole LC/MS electrospray system housed at the National Institute for Environmental Studies, Japan). The UV−vis absorption spectra of ozonolysis reaction mixtures were measured with an Agilent 8453 UV−vis spectrophotometer. All experiments were performed at 298 ± 1 K.

Online negative-ion electrospray mass spectrometry of solutions containing submillimolar amounts of NaCl was used to detect chloride (Cl^-) adducts of α-HHs and other products.[1,9] We previously showed that compounds possessing at least three functional groups including a peroxide (−OOH or −OOR) moiety, an alcohol (−OH) moiety, and a ketone (−RC═O) moiety form Cl^- adducts and are detectable as $[M + Cl]^-$.[20,21] The temporal profiles of the ion signals for Cl^- adducts of α-HHs and other reactants and products were determined with the electrospray mass spectrometer and a digital stopwatch.

The total concentration of peroxides including H_2O_2 accumulated after the ozonation of a solution (α-Tp + NaCl) was evaluated by iodometry. From the time-dependent UV−vis absorption spectra of aqueous solution of 50 mM NaI + 0.1 mM HCl + 0−0.05 mM H_2O_2 recorded until the absorption of I_3^- at 350 nm reached a plateau value, we obtained a linear correlation between the absorbance at 350 nm (A_{350nm}) and [H_2O_2] (Figure S2). By substituting A_{350nm} obtained from an aliquot of a solution of 1 mM α-Tp + 0.2 mM NaCl + 0.06 mM O_3 + 0.1 mM HCl at 4−5 h after ozonation plus 50 mM NaI, we estimated the peroxides in the solution.

The following conditions were used for the electrospray mass spectrometer: dry nitrogen gas flow rate, 12 L min^{-1}; dry nitrogen gas temperature, 340 °C; inlet voltage, +3.5 kV relative to ground; and fragmentor voltage, 60 V. All solutions were prepared in purified water (resistivity, ≥18.2 MΩ cm at 298 K) prepared with a Milli-Q water purification system (Merck, Direct-Q 3UV) and were used within several hours of preparation.

The following chemicals were used as received: α-terpineol (>95%, Tokyo Chemical Industry), terpinen-4-ol (>95%, Tokyo Chemical Industry), $FeCl_2{\cdot}4H_2O$ (≥99.0%, Wako), $FeCl_3{\cdot}6H_2O$ (≥99.9%, Wako), $FeSO_4{\cdot}7H_2O$ (≥99.0%, Wako),

https://doi.org/10.1021/acs.est.1c04635
Environ. Sci. Technol. 2021, 55, 12893−12901

$ZnCl_2$ (≥99.9%, Wako), $CuCl_2{\cdot}2H_2O$ (≥99.0%, Nacalai Tesque), NaI (≥99.999%, Sigma-Aldrich), DMSO (≥99.9%, Sigma-Aldrich), H_2O_2 (30 wt %, Wako), 0.1 M phosphate buffer (Na_2HPO_4/KH_2PO_4, pH 7.4 at 293 K, Nacalai Tesque), 0.1 M acetate buffer solution (CH_3CO_2H/CH_3CO_2Na, pH 5.0 at 293 K, Nacalai Tesque), and NaCl (≥99.999%, Sigma-Aldrich).

3. RESULTS AND DISCUSSION

3.1. Ozonolysis Reactions in the Absence of pH Buffers. We measured the negative-ion mass spectra of ozonolysis reaction mixtures containing O_3(aq), α-Tp/NaCl(aq), and 0.05 mM $FeCl_2$(aq) at pH 4.0−4.1 at 5, 9, 25, and 60 min after addition of the iron solution (Figure 1).

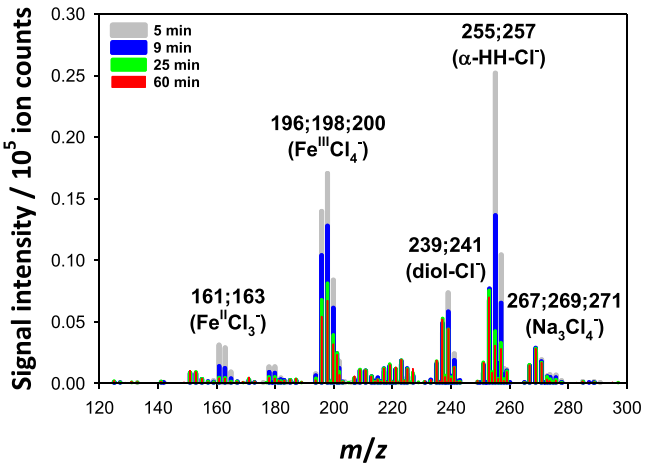

Figure 1. Time-dependent negative-ion mass spectra of mixtures of 1 mM α-Tp, 0.2 mM NaCl, 0.06 mM O_3, and 0.05 mM $FeCl_2$ in water at pH 4.0−4.1. The signals at m/z 161;163 and 196;198;200 correspond to $Fe^{II}Cl_3^-$ and $Fe^{III}Cl_4^-$, respectively. The signals at m/z 255;257 and 239;241 correspond to Cl^- adducts of α-HHs and geminal diols, respectively. The signal at m/z 267;269;271 corresponds to $Na_3Cl_4^-$.

Ozone reacts with α-Tp to produce a primary ozonide,[9,24] which isomerizes to CIs in solution; the CIs then isomerize or react with $(H_2O)_{n\geq1}$ in bulk water to produce α-HH-Cl^- adducts[20,21,25] (Scheme 1). The doublet at m/z 255;257 shown in Figure 1 was assigned to the α-HH-Cl^- adducts derived from α-Tp: 255;257 = 154 (α-Tp) + 48 (O_3) + 18 (H_2O) + 35;37 (Cl^-).[11,20] The signal at m/z 239;241 was assigned to Cl^- adducts of the geminal diols produced by decomposition of α-HHs.[19] Additional details regarding peak assignments of these products on the basis of experiments in D_2O and $H_2{}^{18}O$ can be found in our previous study.[20] It is noted that since we could only detect specific products bearing at least three functional groups as their chloride adducts, other products such as secondary ozonide (SOZ) that likely formed via the isomerization of CIs[22] would be mass spectrometry-silent. The signals at m/z 161;163(;165) and 196;198;200 were attributed to $Fe^{II}Cl_3^-$ and $Fe^{III}Cl_4^-$, respectively. Note that Fe^{2+} and Fe^{3+} exist as $Fe^{2+}(H_2O)_6$ and $Fe^{3+}(H_2O)_6$, respectively, in bulk water, which are detected as $FeCl_3^-$ and $FeCl_4^-$ by the mass spectrometer. The m/z 267;269;271 signal was attributed to $Na_3Cl_4^-$, and as expected, this signal did not change with time. Signals at m/z 253;255 and m/z 237;239 were observed even when the α-Tp and $FeCl_2$ solutions were mixed in the absence of O_3 (conditions under which no α-HHs formed) and persisted throughout the measurement period (Figure S3), implying that they can be attributed to Cl^- adducts of relatively inert reaction products formed by autoxidation of α-Tp in the presence of Fe^{2+} (and dissolved O_2).

Solutions of $FeCl_2$ are acidic, and addition of 0.05 mM $FeCl_2$ decreased the pH to approximately 4. At pH 4.0−4.1, the α-HH-Cl^- and geminal diol-Cl^- signals rapidly decayed with time, which is consistent with previous results.[19] We have proposed that α-HHs undergo H^+-catalyzed conversion into the corresponding aldehydes and H_2O_2 in acidic water.[26] The aldehydes can be hydrated to form the observed geminal diols, or they can isomerize to form mass spectrometry-silent lactols. An iodometry analysis of a mixture of 1 mM α-Tp + 0.2 mM NaCl + 0.06 mM O_3 + 0.1 mM HCl in the absence of $FeCl_2$ at

Scheme 1. Formation and Decomposition of α-Hydroxyalkyl-Hydroperoxides in Acidic Water in the Presence of Ferrous Ions[a]

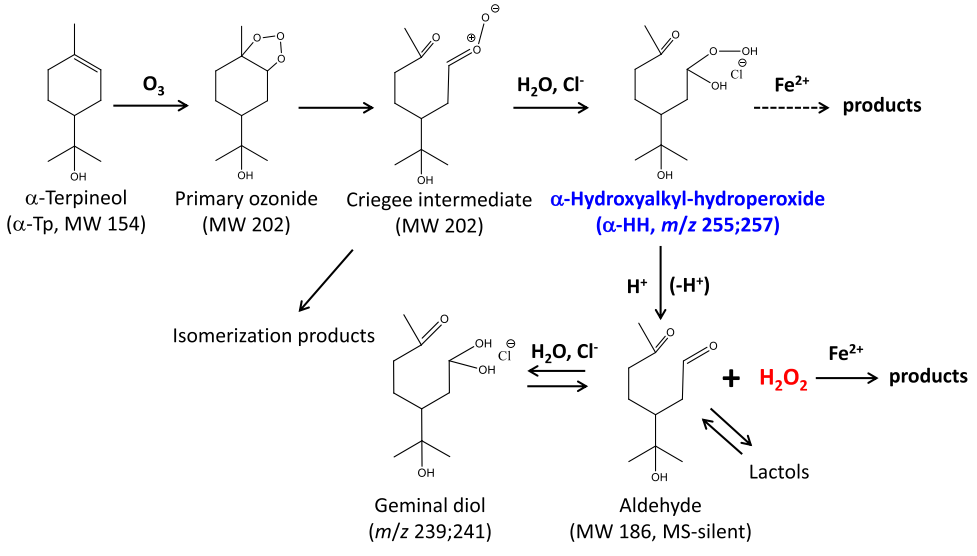

[a]The likely structural isomers are shown.

https://doi.org/10.1021/acs.est.1c04635
Environ. Sci. Technol. 2021, 55, 12893−12901

4−5 h after ozonation indicates that the total concentration of peroxides is 0.04 ± 0.01 mM (derived from three ozonolysis experiments). Note that since α-HHs should have completely decomposed into H_2O_2 in water at pH ∼ 4 at 4−5 h, this is the total concentration of H_2O_2 and mass spectrometry-silent peroxides (e.g., SOZ). Interestingly, the result implies that ∼70% of O_3 was converted into H_2O_2 and other peroxides in the mixture of α-Tp + NaCl solution under the present condition.

The Fe^{II} and Fe^{III} signals also decayed as a function of time, results that are attributed to the reaction of Fe^{2+} with H_2O_2 produced by H^+-catalyzed decomposition of α-HHs and hydrolysis of Fe^{3+}, respectively (see below). Note that $FeCl_2$ was added to the solution after all the O_3 had reacted with α-Tp, and therefore, no reaction of Fe^{2+} with O_3 occurred (see Materials and Methods). The lack of new product signals in the mass spectra upon addition of $FeCl_2$ suggests two possibilities: either the reaction of α-HHs with Fe^{2+} was too slow to compete with H^+-catalyzed decomposition or the reaction produced RO radicals that were transformed into mass spectrometry-silent products. Results discussed below indicate that the former is more likely to occur.

We also measured the UV−vis absorption spectra of an aqueous reaction mixture containing α-Tp (1 mM), NaCl (0.2 mM), O_3 (0.06 mM), and $FeCl_2$ (0.01 mM) at pH 4.7−5.1 as a function of reaction time (Figure S4). The prominent peak at 197 nm, which originates from the $\pi-\pi^*$ transition of the C=C double bond of α-Tp, did not change with time once the ozonation occurred. The absence of new peaks and the stability of the UV−vis spectrum over the course of 161 min indicate that the α-HHs, geminal diols, and Fe^{II}/Fe^{III}-containing complexes produced during the reaction did not absorb strongly in the wavelength region from 190 to 700 nm. The fact that the peak at 197 nm did not change also demonstrates that no radical chain reactions, which would have decreased the concentration of α-Tp, occurred in this system.[27]

Next, we used mass spectrometry to analyze the ozonolysis reaction of α-Tp in aqueous solutions containing dimethylsulfoxide (DMSO) because conversion of DMSO into methanesulfonate (MSA^-) can be used as an indicator of OH-radical formation. In aqueous solution, DMSO is known to react with OH radicals ($k = 4.5 \times 10^9\ M^{-1}\ s^{-1}$) to form methanesulfinic acid (and $\cdot CH_3$) in ∼100% yield;[28] methanesulfinic acid then reacts with additional OH radicals to form methanesulfonic acid ($pK_a = -2.6$), which can be detected as MSA^- by mass spectrometry (m/z 95, Scheme 2).[29]

We obtained negative-ion mass spectra of a reaction mixture containing α-Tp, NaCl, O_3, $FeCl_2$, and DMSO and a mixture containing H_2O_2, $FeCl_2$, and DMSO in an aqueous solution (Figure 2).

Reaction of the H_2O_2 + $FeCl_2$ + DMSO mixture yielded a substantial amount of MSA^- (Figure 2B), implying that the

Scheme 2. Formation of MSA^- by Reaction of DMSO with OH Radicals

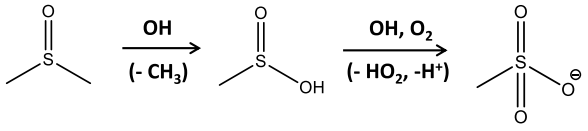

Dimethylsulfoxide (DMSO, MW 78) | Methanesulfinic acid (MW 80) | **Methanesulfonate** (MSA^-, m/z 95)

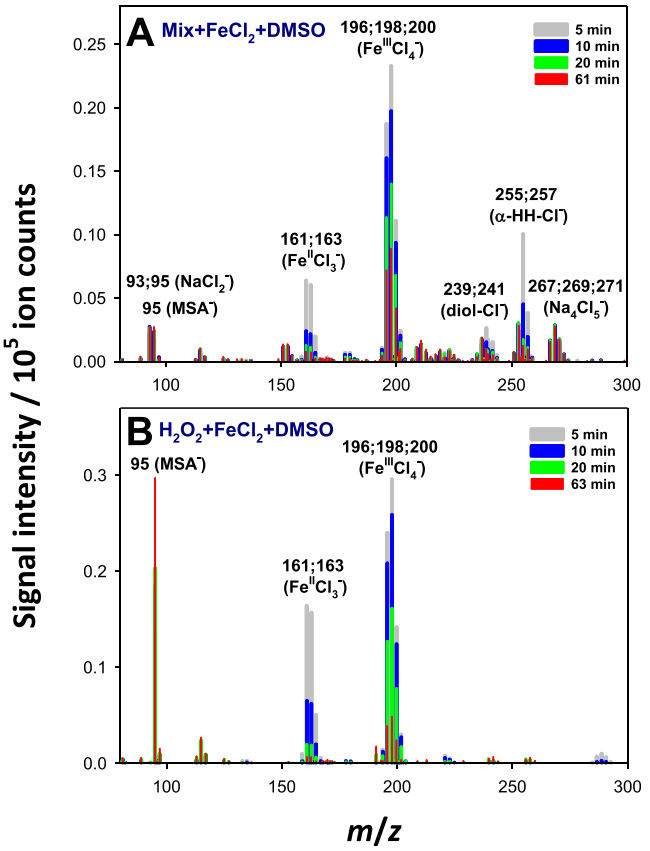

Figure 2. Time-dependent negative-ion mass spectra of (A) a mixture of 1 mM α-Tp, 0.2 mM NaCl, O_3 ($[O_3]_0$ = 0.06 mM), 100 mM DMSO, and 0.05 mM $FeCl_2$ in water at pH 4.0−4.2 and (B) a mixture of 0.05 mM H_2O_2, 100 mM DMSO, and 0.05 mM $FeCl_2$ in water at pH 4.0−4.1. Mix = α-Tp + NaCl + O_3.

Fenton reaction (Fe^{2+} + H_2O_2) in water at pH 4.0−4.1 produced OH radicals in a high yield, which is consistent with previously reported results.[30,31] Although the identity of the reactive intermediates of the Fenton reaction and the rate constant for their formation depend on the pH, coreactants, and water content of the reaction medium,[30,32−34] it is generally accepted that the reaction produces OH radicals in acidic bulk water. We observed only a limited yield of MSA^- from reaction of the α-Tp + NaCl + O_3 + $FeCl_2$ + DMSO mixture (Figure 2A). Note that the MSA^- signal at m/z 95 partly overlapped with the $NaCl_2^-$ cluster signal at m/z 93;95. The formation of a nonzero amount of MSA^- implies secondary formation of OH radicals by a reaction between Fe^{2+} and H_2O_2, which was gradually produced by H^+-catalyzed decomposition of the α-HHs (Scheme 1). It has been shown that H^+-catalyzed decomposition of α-HHs generates H_2O_2 and the process preserves the −OOH moiety.[26] Thus, even if α-HHs did not directly react with Fe^{2+}, H_2O_2 formed by this mechanism could have reacted with Fe^{2+} in the acidic water solution to produce OH radicals.

Next, we plotted the temporal profiles of the reactant and product signals for reactions of the α-Tp + NaCl + O_3 + $FeCl_2$ + DMSO mixture and the H_2O_2 + $FeCl_2$ + DMSO mixture (Figure 3).

The MSA^- signal for the reaction of the α-Tp + NaCl + O_3 + $FeCl_2$ + DMSO mixture increased continuously throughout the measurement period (Figure 3A), whereas the MSA^- signal for the reaction of the H_2O_2 + $FeCl_2$ + DMSO mixture

https://doi.org/10.1021/acs.est.1c04635
Environ. Sci. Technol. 2021, 55, 12893−12901

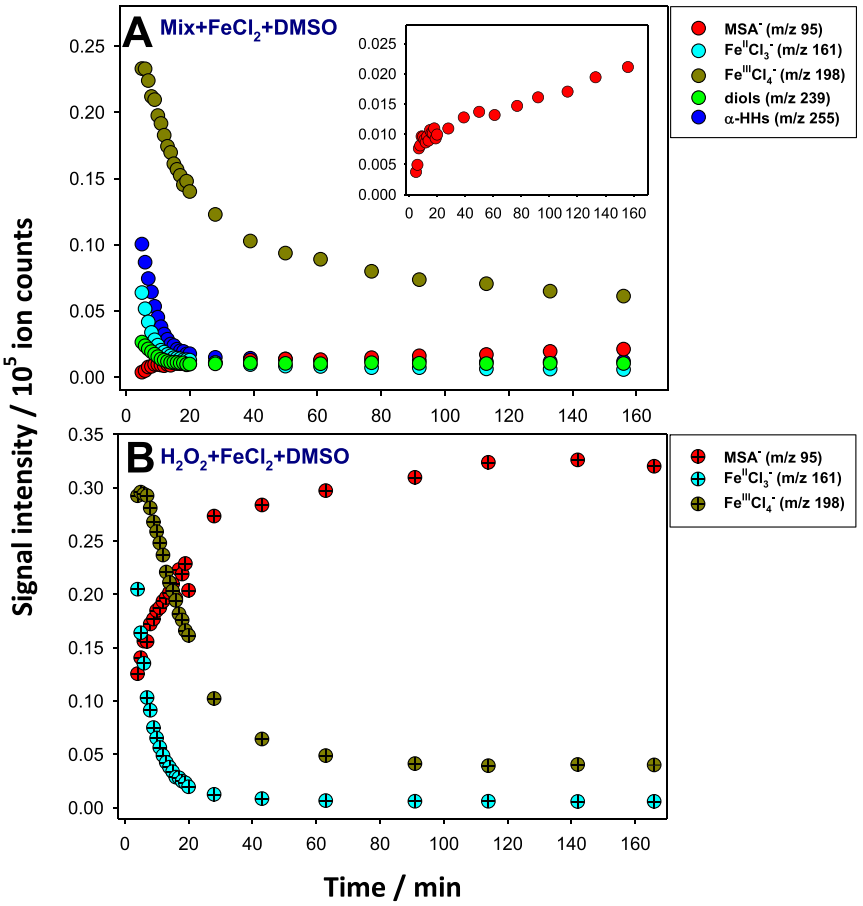

Figure 3. (A) Temporal profiles of the signals for reactants and products of a reaction of 1 mM α-Tp, 0.2 mM NaCl, 0.06 mM O_3, 100 mM DMSO, and 0.05 mM $FeCl_2$ in water at pH 4.0–4.2. The inset shows the enlarged temporal profile of the MSA^- (m/z 95) signal. The contribution of the $NaCl_2^-$ signal (m/z 93;95 and signal intensity ratio, 1.00:0.64) was subtracted from that of the MSA^- signal. Mix = α-Tp + NaCl + O_3. (B) Temporal profiles of the signals for the reactants and products of a reaction of H_2O_2 (0.05 mM), DMSO (100 mM), and $FeCl_2$ (0.05 mM) in water at pH 4.0–4.1.

appeared to reach a plateau (Figure 3B). The plateau indicates that 0.05 mM H_2O_2 was consumed by Fe^{2+}/Fe^{3+} within ~160 min. At ~160 min, the intensity of the MSA^- signal in Figure 3A was 5.7 ± 0.8% of the signal in Figure 3B (derived from three sets of experiments), indicating that the amount of OH radicals formed in the α-Tp + NaCl + O_3 + $FeCl_2$ + DMSO mixture was much smaller than the amount formed in the H_2O_2 + $FeCl_2$ + DMSO mixture. The MSA^- signal for the α-Tp + NaCl + O_3 + $FeCl_2$ + DMSO mixture rapidly evolved at the beginning of the reaction (<10 min) and increased slowly and monotonically thereafter (Figure 3A, inset). The rapid increase is attributed to the reaction of Fe^{2+} with H_2O_2 formed via H^+-catalyzed decomposition of α-HHs, and the slow increase may be attributed to the reaction between Fe^{3+} and mass spectrometry-silent products (e.g., SOZ). Notably, at a period >20 min, Fe^{2+} and α-HHs already disappeared, while Fe^{3+} persisted (Figure 3A). Since the reaction of Fe^{3+} with H_2O_2 is reported to be several orders of magnitude slower than that of Fe^{2+} with H_2O_2,[34,35] other peroxides such as SOZ would contribute to the observed slow OH formation. To fully elucidate the underlying reaction mechanisms, further investigations including quantification of SOZ will be necessary. Because the $Fe^{III}Cl_4^-$ signal decayed slowly even in the absence of ozone (i.e., in the absence of α-HHs; Figure S3), the decay of Fe^{III} observed in Figure 3A is partly attributed to the hydrolysis of Fe^{3+}: $Fe^{3+} + 3H_2O \rightleftarrows Fe(OH)_3 + 3H^+$ and $Fe^{3+} + 3OH^- \rightarrow Fe(OH)_3$. Because the UV–vis spectra were unchanged during the measurement of α-Tp + NaCl + O_3 + $FeCl_2$ mixture (Figure S4), we assumed that the formation of colloidal $Fe(OH)_3$ did not affect the results. The decrease in pH from 4.2 to 4.0 during the measurement is consistent with the abovedescribed mechanism. Note that Fe^{2+} was not hydrolyzed under the present conditions (Figure S3).

Although we cannot completely exclude the possibility that the reaction of α-HHs with Fe^{2+}/Fe^{3+} directly produced a limited amount of OH radicals, investigation of the reaction kinetics showed this possibility to be unlikely (see below). In this context, we note a previous report showing that the reactions of both CH_3OOH and C_2H_5OOH with Fe^{2+} in water at pH 2 and 279 K produce the corresponding RO radicals, rather than OH radicals.[17] The rate constants for these two reactions were reported to be 16 ± 5 and 24 ± 9 M^{-1} s^{-1}, respectively; the rate constants for reaction of Fe^{2+} with α-HHs derived from α-Tp and other terpenes have not been reported.

The observed decay of the $Fe^{II}Cl_3^-$ signal from the reaction of the H_2O_2 + $FeCl_2$ + DMSO mixture within 20 min (Figure 3B) is consistent with the consumption of Fe^{2+} (0.05 mM) by H_2O_2 (0.05 mM) (the Fenton reaction) with a rate constant of ~60 M^{-1} s^{-1}.[32] The rise-and-decay behavior observed for the $Fe^{III}Cl_4^-$ signal is consistent with conversion of Fe^{2+} to Fe^{3+} by the Fenton reaction and subsequent slow hydrolysis of Fe^{3+}.

https://doi.org/10.1021/acs.est.1c04635
Environ. Sci. Technol. 2021, 55, 12893–12901

Note that in the absence of a buffer, the pH of the α-Tp + NaCl + O_3 + $FeCl_2$ + DMSO mixture decreased from 4.2 at 8 min to 4.0 at 20 min. Because the rates of α-HH and Fe^{2+}/Fe^{3+} decay vary with even slight changes in pH,[19,30] we need to quantitatively analyze the reaction kinetics under pH-controlled conditions, so we carried out reactions of α-HHs with metal ions in the presence of two different pH buffers.

3.2. Ozonolysis Reactions in the Presence of pH Buffers. To investigate the effects of pH, we carried out separate ozonolysis reactions of mixtures in an acetate buffer (pH 5.1) and a phosphate buffer (pH 7.6). Figure S5 shows the time-dependent mass spectra of 1 mM α-Tp, 0.2 mM NaCl, 0.06 mM O_3, and 1 mM acetate buffer in the absence and presence of 0.05 mM $FeCl_2$ in water at pH 5.1 ± 0.1. In the presence of 1 mM acetate (A^-), both α-HH-Cl^- (m/z 255;257) and α-HH-A^- [m/z = 279 = 154 (α-Tp) + 48 (O_3) + 18 (H_2O) + 59 (acetate)] were detected. We confirmed that the decay profiles of the α-HH-Cl^- and α-HH-A^- signals were the same within experimental uncertainties (Figure S6). We observed no evidence for the formation of new products of α-HH oxidation/decomposition in the mass spectra upon addition of $FeCl_2$, which is consistent with the results of the experiments in the absence of pH buffers. In the presence of excess acetate ([A^-] = 1 mM > [$FeCl_2$] = 0.05 mM), the intensities of the A^- and $NaA_2^-/Na_2A_3^-$ cluster signals remained constant over time (Figure S5). The result indicates that chain reactions involving OH radicals do not occur under these conditions; the formation of OH radicals would have resulted in a decrease in the A^- signal.

We also compared the decay profiles of the α-HH-Cl^- signals (m/z 255) for a mixture of α-Tp, NaCl, O_3, and acetate buffer in the absence and presence of $FeCl_2$, $ZnCl_2$, $CuCl_2$, or $FeCl_3$ (0.05 mM) in water at pH 5.1 ± 0.1 (Figure 4). All the profiles were well fitted by the single-exponential decay function $S = S_0 \exp(-kt)$, from which we calculated first-order rate constants (k) and lifetimes ($\tau_{1/e}$, Table 1).

In the presence of the metal ions, the pH decreased slightly (from 5.1 to 5.0) during the measurement period, even in a 5 mM acetate buffer solution. For example, the pH of a solution

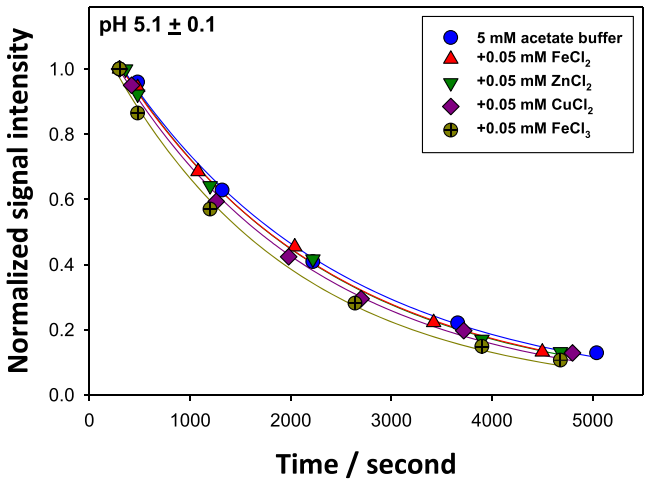

Figure 4. Temporal profiles of α-HH-Cl^- signals (m/z 255) during reactions of mixtures of 1 mM α-Tp, 0.2 mM NaCl, O_3 ($[O_3]_0$ = 0.06 mM), and 5 mM acetate buffer in the absence or presence of 0.05 mM metal salts in water at pH 5.1 ± 0.1 (pH 5.0 ± 0.1 for $FeCl_3$). Curves show fits to a single-exponential decay function: $S = S_0 \exp(-kt)$. See the text for details.

Table 1. Rate Constants (k) and Lifetimes ($\tau_{1/e}$) for Decay of Signals for α-HHs Derived from Aqueous-Phase Ozonolysis of α-Tp and Terpinen-4-ol in the Presence of a 5 mM Acetate Buffer (pH 5.1 ± 0.1) and in the Absence or Presence of Metal Salts

α-HHs	dopant	$k_{pH5.1}$ (s^{-1})[a]	$\tau_{1/e}$ (min)
α-Tp α-HHs	no metal	$(4.5 \pm 0.1) \times 10^{-4}$	37
	0.02 mM $FeCl_2$	$(4.7 \pm 0.2) \times 10^{-4}$	35
	0.05 mM $FeCl_2$	$(4.7 \pm 0.2) \times 10^{-4}$	35
	0.05 mM $FeSO_4$	$(4.7 \pm 0.1) \times 10^{-4}$	35
	0.05 mM $ZnCl_2$	$(4.7 \pm 0.1) \times 10^{-4}$	35
	0.05 mM $CuCl_2$	$(4.8 \pm 0.2) \times 10^{-4}$	35
	0.05 mM $FeCl_3$	$(5.5 \pm 0.2) \times 10^{-4}$[b]	30
terpinen-4-ol α-HHs[c]	no metal	$(1.4 \pm 0.1) \times 10^{-4}$	119
	0.05 mM $FeCl_2$	$(1.6 \pm 0.2) \times 10^{-4}$	104

[a]Errors indicate standard deviations of three independent experiments. [b]The pH for this experiment was 5.0 ± 0.1. [c]Values were determined from the α-HH-A^- adduct signals.

containing 0.05 mM $CuCl_2$ gradually decreased from 5.1 at 7 min to 5.0 at 80 min. In addition, the solution containing 0.05 mM $FeCl_3$ was at pH 5.0 from the beginning of the kinetics experiment; we attributed this rapid 0.1 pH unit decrease to the slightly faster decay observed for the reaction in the presence of $FeCl_3$. We also measured the temporal profile of the α-HH-Cl^- signal in the presence of 0.05 mM $FeSO_4$ (Table 1) to confirm that the counter ion of the metal salt did not influence the kinetics.

In addition, we measured the temporal profiles of the terpinen-4-ol α-HH-A^- signal at m/z 279 in the absence and presence of $FeCl_2$. In a previous study, we found that the decay of terpinen-4-ol α-HHs in water is much slower than the decay of α-Tp α-HHs.[19] We used the α-HH-A^- signal to calculate the rate constants because its intensity was larger than that of the α-HH-Cl^- signal in the experiments involving terpinen-4-ol. The k values determined for the decay of terpinen-4-ol α-HHs in the absence and presence of 0.05 mM $FeCl_2$ were $(1.4 \pm 0.1) \times 10^{-4}$ and $(1.6 \pm 0.2) \times 10^{-4}$ s^{-1} at pH 5.1 ± 0.1, respectively. In all cases, k was slightly larger in the presence of metal ions than in their absence (Table 1). The fact that identical k values were obtained with 0.02 and 0.05 mM $FeCl_2$ implies that the direct reaction of α-HHs with Fe^{2+} did not occur.

As we reported previously, k is very sensitive to pH, increasing with decreasing pH.[19] By analyzing the previously reported data on the pH dependency of k determined from the decay of α-Tp α-HHs in the absence of metal ions in the pH range from 3.0 to 6.1 (Figure S7),[19] we derived the following function for the correlation between k and pH: $\ln k = 1.166 (\pm 0.280) - 1.681 (\pm 0.058) \times \text{pH}$. This correlation suggests that a ΔpH of −0.1 (i.e., a change from 5.1 to 5.0) would increase k by ∼18%, which could explain the observed increase in k upon the addition of metal salt solutions. This reasoning is consistent with our finding that the largest k was observed in the $FeCl_3$ experiment in which the pH was 5.0 immediately after the start of the kinetics experiment. Other metal ions decreased the solution pH from 5.1 to 5.0 gradually, over the course of 80 min.

Thus, we attribute the slightly larger k obtained in the experiments involving metal ions to the slight pH decrease rather than to a direct reaction of α-HHs with metal ions or to

https://doi.org/10.1021/acs.est.1c04635
Environ. Sci. Technol. 2021, 55, 12893−12901

metal-catalyzed decomposition of α-HHs. This conclusion is consistent with the results of our experiments in the absence of pH buffers.

Finally, we investigated the effects of metal ions on α-HH decay in water at pH 7.6 ± 0.2. The temporal profiles of the α-HH-Cl^- signals (m/z 255) for mixtures of α-Tp, NaCl, O_3, and phosphate buffer in the absence and presence of $FeCl_2$, $ZnCl_2$, $CuCl_2$, or $FeCl_3$ in water at pH 7.6 ± 0.2 are shown in Figure 5.

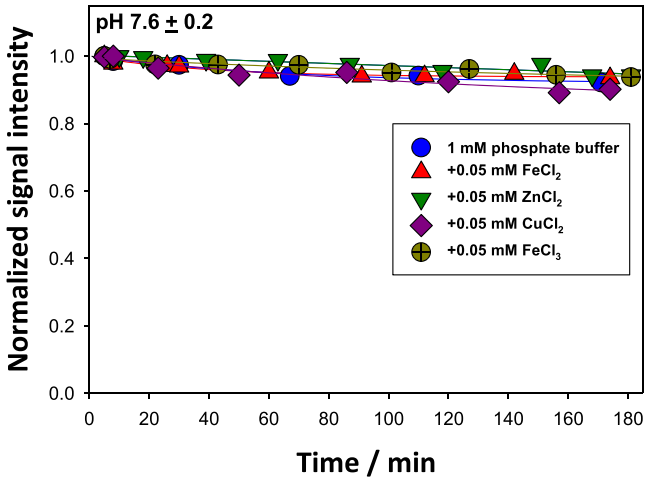

Figure 5. Temporal profiles of α-HH-Cl^- signals (m/z 255) for mixtures of 1 mM α-Tp, 0.2 mM NaCl, O_3 ($[O_3]_0$ = 0.06 mM), and 1 mM phosphate buffer in the absence or presence of 0.05 mM metal salts in water at pH 7.6 ± 0.2. The curves are a guide to the eye.

The profiles clearly indicated that the effects of metal ions on the decay of α-Tp α-HHs in water at pH 7.6 were negligible, which is consistent with the plots shown in Figure 4 and with our conclusion that pH, rather than the presence of metal ions, was the critical determinant of the lifetime of α-HHs derived from the terpene alcohols used in this study. We can infer that the same conclusion may be drawn for other structurally similar cyclic terpenes such as α-pinene and limonene.

We also measured time-dependent UV−vis absorption spectra of a mixture of 1 mM α-Tp, 0.2 mM NaCl, 0.06 mM O_3, and 0.05 mM $FeCl_2$ in phosphate buffer (1 mM) at pH 7.6 ± 0.2 and found that no new peaks in the wavelength range from 190 to 700 nm evolved within 240 min (Figure S8), which is consistent with our results for experiments in the absence of pH buffers (Figure S4).

4. ATMOSPHERIC IMPLICATIONS

Chevallier et al. have reported that reactions of ROOHs (R = CH_3 or C_2H_5) and Fe^{2+} produce Fe^{3+}, RO·, and OH^- in water at 279 K and pH 2.[17] In this study, we showed that the decomposition of α-HHs derived from ozonolysis of two C_{10} terpenoids was not influenced by the presence of Fe^{2+}, Zn^{2+}, Cu^{2+}, or Fe^{3+} at concentrations of ≤50 μM. Our results suggest that in atmospheric aqueous phases that are generally acidic, H^+-catalyzed decomposition of α-HHs is much faster than the reactions of α-HHs with these metal ions. We note that the typical concentrations of metal ions in atmospheric aqueous phases can be expected not to exceed 5 μM, whereas $[H^+]$ exceeds 100 μM (i.e., pH ≤ 4). As a reference, atmospheric aerosol particles collected in Baltimore, Maryland, were shown to have a pH of ≤2, indicating a $[H^+]/[Fe^{2+}]$ ratio of >2 × 10^3.[12] In addition, PM_1 sampled during the CalNex campaign in Pasadena, California, was shown to have a similar pH (1.9 ± 0.5).[36] Because the lifetime of the α-Tp α-HHs in aqueous aerosols at pH 2 is estimated to be just a few seconds, we conclude that H^+-catalyzed decomposition in atmospheric acidic aqueous media is much faster than degradation by other processes. The UV−vis spectra of the reaction mixtures obtained in this study suggest that solar photolysis is not an important decomposition pathway of α-Tp α-HHs in aqueous aerosols under ambient conditions (Figures S4 and S8). The results of a recent chamber study revealed that peroxide groups are not the main photolabile groups in SOAs generated from α-pinene ozonolysis.[37]

Our present results suggest that OH radicals can be formed by reaction of Fe^{2+} with H_2O_2 produced by H^+-catalyzed decomposition of α-HHs, rather than by direct reaction of Fe^{2+} with α-HHs under atmospherically relevant conditions (i.e., $[Fe^{2+}] \approx [\alpha\text{-HHs}] < 50\ \mu M$). Importantly, H_2O_2 is produced not only by H^+-catalyzed decomposition of α-HHs but also by decomposition of α-acyloxyalkyl-hydroperoxides,[38] α-alkoxyalkyl-hydroperoxides,[11] and likely highly oxygenated organic molecules (HOMs) in aqueous media.[1,38] Recent field measurements revealed that the decomposition of organic peroxides is the dominant source of aerosol-phase H_2O_2.[39,40] Thus, our results shed new light on the mechanism of formation of radicals in particulate matter-dissolved water reported in the literature.[41,42] To reveal the effects of functionalities of ROOHs (e.g., single vs multiple -OOH) on the decomposition mechanism, further investigation is necessary.

Finally, we note that inhalation of metal ions combined with aerosols containing H_2O_2 produced by conversion of α-HHs into H_2O_2 could cause extensive oxidation of antioxidants and lipid surfactants and proteins of the epithelium-lining fluid of the pulmonary alveoli.[43−46]

■ ASSOCIATED CONTENT

Supporting Information

The Supporting Information is available free of charge at https://pubs.acs.org/doi/10.1021/acs.est.1c04635.

Additional experimental data, including the schematic setup and procedure, time-dependent mass spectra of α-terpineol + NaCl + O_2 + $FeCl_2$, UV−vis spectra obtained from α-terpineol + NaCl + O_3 + $FeCl_2$ in the absence/presence of pH buffers, and plot of natural logarithm of the rate constants (ln k) for decay of the α-HHs generated by ozonolysis of aqueous α-terpineol versus pH (PDF)

■ AUTHOR INFORMATION

Corresponding Author

Shinichi Enami − *National Institute for Environmental Studies, Tsukuba 305-8506, Japan;* orcid.org/0000-0002-2790-7361; Phone: +81-29-850-2770; Email: enami.shinichi@nies.go.jp

Authors

Mingxi Hu − *Graduate School of Frontier Sciences, The University of Tokyo, Kashiwa 277-8563, Japan*

Kenichi Tonokura − *Graduate School of Frontier Sciences, The University of Tokyo, Kashiwa 277-8563, Japan;* orcid.org/0000-0003-1910-8508

Yu Morino − *National Institute for Environmental Studies, Tsukuba 305-8506, Japan;* orcid.org/0000-0003-3344-3986

Kei Sato − *National Institute for Environmental Studies, Tsukuba 305-8506, Japan;* orcid.org/0000-0002-3716-3730

Complete contact information is available at: https://pubs.acs.org/10.1021/acs.est.1c04635

Author Contributions

S.E. designed the research; M.H. and S.E. performed the experiments; S.E. wrote the first draft of the manuscript; all the authors analyzed the data and contributed to the revisions of the manuscript.

Notes

The authors declare no competing financial interest.

■ ACKNOWLEDGMENTS

S.E. is grateful for a KAKENHI grant from the Japan Society for the Promotion of Science (no. 19H01154). This research was partly supported by an NIES research funding (Type A).

■ REFERENCES

(1) Enami, S. Fates of Organic Hydroperoxides in Atmospheric Condensed Phases. *J. Phys. Chem. A* **2021**, *125*, 4513−4523.
(2) Bonn, B.; von Kuhlmann, R.; Lawrence, M. G. High contribution of biogenic hydroperoxides to secondary organic aerosol formation. *Geophys. Res. Lett.* **2004**, *31*, 4.
(3) Anglada, J. M.; Martins-Costa, M.; Francisco, J. S.; Ruiz-López, M. F. Interconnection of Reactive Oxygen Species Chemistry across the Interfaces of Atmospheric, Environmental, and Biological Processes. *Acc. Chem. Res.* **2015**, *48*, 575−583.
(4) Jr-Min Lin, J.; Chao, W. Structure-dependent reactivity of Criegee intermediates studied with spectroscopic methods. *Chem. Soc. Rev.* **2017**, *46*, 7483−7497.
(5) Long, B.; Bao, J. L.; Truhlar, D. G. Rapid unimolecular reaction of stabilized Criegee intermediates and implications for atmospheric chemistry. *Nat. Commun.* **2019**, *10*, 2003.
(6) Vereecken, L.; Novelli, A.; Taraborrelli, D. Unimolecular decay strongly limits the atmospheric impact of Criegee intermediates. *Phys. Chem. Chem. Phys.* **2017**, *19*, 31599−31612.
(7) Zhou, Z.; Abbatt, J. P. D. Formation of Gas-Phase Hydrogen Peroxide via Multiphase Ozonolysis of Unsaturated Lipids. *Environ. Sci. Technol. Lett.* **2021**, *8*, 114−120.
(8) Heine, N.; Houle, F. A.; Wilson, K. R. Connecting the Elementary Reaction Pathways of Criegee Intermediates to the Chemical Erosion of Squalene Interfaces during Ozonolysis. *Environ. Sci. Technol.* **2017**, *51*, 13740−13748.
(9) Enami, S.; Colussi, A. J. Criegee Chemistry on Aqueous Organic Surfaces. *J. Phys. Chem. Lett.* **2017**, *8*, 1615−1623.
(10) Zhou, X.; Lee, Y. N. Aqueous solubility and reaction kinetics of hydroxymethyl hydroperoxide. *J. Phys. Chem.* **1992**, *96*, 265−272.
(11) Hu, M.; Qiu, J.; Tonokura, K.; Enami, S. Aqueous-phase fates of α-alkoxyalkyl-hydroperoxides derived from the reactions of Criegee intermediates with alcohols. *Phys. Chem. Chem. Phys.* **2021**, *23*, 4605−4614.
(12) Pye, H. O. T.; Nenes, A.; Alexander, B.; Ault, A. P.; Barth, M. C.; Clegg, S. L.; Collett, J. L., Jr.; Fahey, K. M.; Hennigan, C. J.; Herrmann, H.; Kanakidou, M.; Kelly, J. T.; Ku, I. T.; McNeill, V. F.; Riemer, N.; Schaefer, T.; Shi, G.; Tilgner, A.; Walker, J. T.; Wang, T.; Weber, R.; Xing, J.; Zaveri, R. A.; Zuend, A. The acidity of atmospheric particles and clouds. *Atmos. Chem. Phys.* **2020**, *20*, 4809−4888.
(13) Huang, J.; Jones, A.; Waite, T. D.; Chen, Y.; Huang, X.; Rosso, K. M.; Kappler, A.; Mansor, M.; Tratnyek, P. G.; Zhang, H. Fe(II) Redox Chemistry in the Environment. *Chem. Rev.* **2021**, *121*, 8161−8233.
(14) Deguillaume, L.; Leriche, M.; Monod, A.; Chaumerliac, N. The role of transition metal ions on HO_x radicals in clouds: a numerical evaluation of its impact on multiphase chemistry. *Atmos. Chem. Phys.* **2004**, *4*, 95−110.
(15) Furukawa, T.; Takahashi, Y. Oxalate metal complexes in aerosol particles: implications for the hygroscopicity of oxalate-containing particles. *Atmos. Chem. Phys.* **2011**, *11*, 4289−4301.
(16) Kuang, X. M.; Gonzalez, D. H.; Scott, J. A.; Vu, K.; Hasson, A.; Charbouillot, T.; Hawkins, L.; Paulson, S. E. Cloud Water Chemistry Associated with Urban Aerosols: Rapid Hydroxyl Radical Formation, Soluble Metals, Fe(II), Fe(III), and Quinones. *ACS Earth Space Chem.* **2020**, *4*, 67−76.
(17) Chevallier, E.; Jolibois, R. D.; Meunier, N.; Carlier, P.; Monod, A. "Fenton-like" reactions of methylhydroperoxide and ethylhydroperoxide with Fe^{2+} in liquid aerosols under tropospheric conditions. *Atmos. Environ.* **2004**, *38*, 921−933.
(18) Sanchez, J.; Myers, T. N. Peroxides and peroxide compounds, organic peroxides. *Kirk-Othmer Encyclopedia of Chemical Technology* **2000**, DOI: 10.1002/0471238961.1518070119011403.a01.
(19) Qiu, J.; Tonokura, K.; Enami, S. Proton-Catalyzed Decomposition of α-Hydroxyalkyl-Hydroperoxides in Water. *Environ. Sci. Technol.* **2020**, *54*, 10561−10569.
(20) Qiu, J.; Liang, Z.; Tonokura, K.; Colussi, A. J.; Enami, S. Stability of Monoterpene-Derived α-Hydroxyalkyl-Hydroperoxides in Aqueous Organic Media: Relevance to the Fate of Hydroperoxides in Aerosol Particle Phases. *Environ. Sci. Technol.* **2020**, *54*, 3890−3899.
(21) Qiu, J.; Ishizuka, S.; Tonokura, K.; Colussi, A. J.; Enami, S. Water Dramatically Accelerates the Decomposition of α-Hydroxyalkyl-Hydroperoxides in Aerosol Particles. *J. Phys. Chem. Lett.* **2019**, *10*, 5748−5755.
(22) Leviss, D. H.; Van Ry, D. A.; Hinrichs, R. Z. Multiphase Ozonolysis of Aqueous α-Terpineol. *Environ. Sci. Technol.* **2016**, *50*, 11698−11705.
(23) Ferre-Aracil, J.; Cardona, S. C.; Navarro-Laboulais, J. Determination and Validation of Henry's Constant for Ozone in Phosphate Buffers Using Different Analytical Methodologies. *Ozone Sci. Eng.* **2015**, *37*, 106−118.
(24) Criegee, R. Mechanism of ozonolysis. *Angew. Chem. Int. Ed.* **1975**, *14*, 745−752.
(25) Qiu, J.; Ishizuka, S.; Tonokura, K.; Sato, K.; Inomata, S.; Enami, S. Effects of pH on Interfacial Ozonolysis of α-Terpineol. *J. Phys. Chem. A* **2019**, *123*, 7148−7155.
(26) Hu, M.; Chen, K.; Qiu, J.; Lin, Y.-H.; Tonokura, K.; Enami, S. Temperature Dependence of Aqueous-Phase Decomposition of α-Hydroxyalkyl-Hydroperoxides. *J. Phys. Chem. A* **2020**, *124*, 10288−10295.
(27) Li, F.; Tang, S.; Tsona, N. T.; Du, L. Kinetics and mechanism of OH-induced α-terpineol oxidation in the atmospheric aqueous phase. *Atmos. Environ.* **2020**, *237*, No. 117650.
(28) Steiner, M. G.; Babbs, C. F. Quantitation of the hydroxyl radical by reaction with dimethyl-sulfoxide. *Arc. Biochem. Biophys.* **1990**, *278*, 478−481.
(29) Enami, S.; Sakamoto, Y.; Hara, K.; Osada, K.; Hoffmann, M. R.; Colussi, A. J. "Sizing" Heterogeneous Chemistry in the Conversion of Gaseous Dimethyl Sulfide to Atmospheric Particles. *Environ. Sci. Technol.* **2016**, *50*, 1834−1843.
(30) Bataineh, H.; Pestovsky, O.; Bakac, A. pH-induced mechanistic changeover from hydroxyl radicals to iron(IV) in the Fenton reaction. *Chem. Sci.* **2012**, *3*, 1594−1599.
(31) Hug, S. J.; Leupin, O. Iron-catalyzed oxidation of arsenic(III) by oxygen and by hydrogen peroxide: pH-dependent formation of oxidants in the Fenton reaction. *Environ. Sci. Technol.* **2003**, *37*, 2734−2742.

(32) Gozzo, F. Radical and non-radical chemistry of the Fenton-like systems in the presence of organic substrates. *J. Mol. Catal. A: Chem.* **2001**, *171*, 1−22.
(33) Enami, S.; Sakamoto, Y.; Colussi, A. J. Fenton chemistry at aqueous interfaces. *Proc. Natl. Acad. Sci. U. S. A.* **2014**, *111*, 623−628.
(34) Fischbacher, A.; von Sonntag, C.; Schmidt, T. C. Hydroxyl radical yields in the Fenton process under various pH, ligand concentrations and hydrogen peroxide/Fe(II) ratios. *Chemosphere* **2017**, *182*, 738−744.
(35) Pignatello, J. J.; Oliveros, E.; MacKay, A. Advanced Oxidation Processes for Organic Contaminant Destruction Based on the Fenton Reaction and Related Chemistry. *Crit. Rev. Environ. Sci. Technol.* **2006**, *36*, 1−84.
(36) Guo, H.; Liu, J.; Froyd, K. D.; Roberts, J. M.; Veres, P. R.; Hayes, P. L.; Jimenez, J. L.; Nenes, A.; Weber, R. J. Fine particle pH and gas-particle phase partitioning of inorganic species in Pasadena, California, during the 2010 CalNex campaign. *Atmos. Chem. Phys.* **2017**, *17*, 5703−5719.
(37) Krapf, M.; el Haddad, I.; Bruns, E. A.; Molteni, U.; Daellenbach, K. R.; Prévôt, A. S.; Baltensperger, U.; Dommen, J. Labile peroxides in secondary organic aerosol. *Chem* **2016**, *1*, 603−616.
(38) Zhao, R.; Kenseth, C. M.; Huang, Y.; Dalleska, N. F.; Kuang, X. M.; Chen, J.; Paulson, S. E.; Seinfeld, J. H. Rapid Aqueous-Phase Hydrolysis of Ester Hydroperoxides Arising from Criegee Intermediates and Organic Acids. *J. Phys. Chem. A* **2018**, *122*, 5190−5201.
(39) Qin, M.; Chen, Z.; Shen, H.; Li, H.; Wu, H.; Wang, Y. Impacts of heterogeneous reactions to atmospheric peroxides: Observations and budget analysis study. *Atmos. Environ.* **2018**, *183*, 144−153.
(40) Xuan, X.; Chen, Z.; Gong, Y.; Shen, H.; Chen, S. Partitioning of hydrogen peroxide in gas-liquid and gas-aerosol phases. *Atmos. Chem. Phys.* **2020**, *20*, 5513−5526.
(41) Vidrio, E.; Phuah, C. H.; Dillner, A. M.; Anastasio, C. Generation of Hydroxyl Radicals from Ambient Fine Particles in a Surrogate Lung Fluid Solution. *Environ. Sci. Technol.* **2009**, *43*, 922−927.
(42) Tong, H. J.; Arangio, A. M.; Lakey, P. S. J.; Berkemeier, T.; Liu, F. B.; Kampf, C. J.; Brune, W. H.; Pöschl, U.; Shiraiwa, M. Hydroxyl radicals from secondary organic aerosol decomposition in water. *Atmos. Chem. Phys.* **2016**, *16*, 1761−1771.
(43) Shiraiwa, M.; Ueda, K.; Pozzer, A.; Lammel, G.; Kampf, C. J.; Fushimi, A.; Enami, S.; Arangio, A. M.; Fröhlich-Nowoisky, J.; Fujitani, Y.; Furuyama, A.; Lakey, P. S. J.; Lelieveld, J.; Lucas, K.; Morino, Y.; Pöschl, U.; Takahama, S.; Takami, A.; Tong, H.; Weber, B.; Yoshino, A.; Sato, K. Aerosol health effects from molecular to global scales. *Environ. Sci. Technol.* **2017**, *51*, 13545−13567.
(44) Enami, S.; Colussi, A. J. OH-Radical Oxidation of Lung Surfactant Protein B on Aqueous Surfaces. *Mass Spectrom.* **2018**, *7*, 1−7.
(45) Kim, H. I.; Kim, H. J.; Shin, Y. S.; Beegle, L. W.; Jang, S. S.; Neidholdt, E. L.; Goddard, W. A.; Heath, J. R.; Kanik, I.; Beauchamp, J. L. Interfacial Reactions of Ozone with Surfactant Protein B in a Model Lung Surfactant System. *J. Am. Chem. Soc.* **2010**, *132*, 2254−2263.
(46) Wei, J.; Fang, T.; Wong, C.; Lakey, P. S. J.; Nizkorodov, S. A.; Shiraiwa, M. Superoxide Formation from Aqueous Reactions of Biogenic Secondary Organic Aerosols. *Environ. Sci. Technol.* **2021**, *55*, 260−270.

https://doi.org/10.1021/acs.est.1c04635
Environ. Sci. Technol. 2021, 55, 12893−12901